ELSEVIER

Journal of Materials Processing Technology 186 (2007) 331–338

Journal of Materials Processing Technology

www.elsevier.com/locate/jmatprotec

Laser deposited TiC/H13 tool steel composite coatings and their erosion resistance

W.H. Jiang [1], R. Kovacevic *

Research Center for Advanced Manufacturing, School of Engineering, Southern Methodist University, 3101 Dyer Street, Dallas, TX 75205, USA

Received 22 January 2006; received in revised form 9 November 2006; accepted 1 December 2006

Abstract

The present work studies the synthesis and performance of TiC/H13 tool steel composite coatings obtained by the laser deposition technique. The effect of laser beam-scanning speeds and the concentrations of TiC in injected powder on the morphologies and microstructures of deposited beads are investigated. The results show that the beam-scanning speeds affect the size and morphology of the beads. During laser processing, TiC melts, and decomposes, and subsequently, a number of fine TiC precipitates form during cooling that are uniformly distributed in the steel matrix. The amount of injected TiC has a strong influence on the morphology and size of the fine TiC precipitates. Unlike ductile steel and hard carbide coatings, the TiC reinforced steel matrix composite coatings exhibit a decreased slurry erosion resistance at intermediate impact angles in the range from 0 to 90°; while at both smaller and larger impact angles, they show an increased slurry erosion resistance. By increasing the concentration of TiC in the composite coatings, their erosion resistance decreases. The composite coating with 40 vol.% TiC shows an excellent erosion resistance at high impact angles.

Keywords: Laser processing; Coating; Composite; TiC; Microstructure; Erosion

1. Introduction

Laser cladding is widely used for creating various surface coatings with a significant thickness that can effectively protect substrates from harsh service conditions. Various coating materials, such as carbides, oxides, nitrides, borides, and their composites, have been developed. These coatings display a high hardness, wear and erosion resistance, corrosion resistance, and heat insulation.

Metal matrix composites (MMCs) as coatings have recently gained interest, because of their excellent combination of ductility and toughness of metallic matrices with high strength and hardness of ceramic reinforcements. Due to its high hardness, melting point, and thermodynamic stability as well as availability, TiC is extensively used as a reinforcing phase in MMCs' coatings, such as Ni-based [1–3] and steel-based composites [4–6]. Due to a relatively low cost, iron and steel as a coating matrix have potential application prospects. Utilizing laser surface alloying, Ariely et al. [4] produced TiC reinforced steel coating on the surface of AlSl 1045 steel, which exhibits a higher hardness. Tassin et al. [5] incorporated TiC into the surface of AlSl 316 L stainless steel by laser processing, which substantially improved sliding wear resistance. Jiang and Mollan [6] increased the life of die-casting dies by laser surface processing with micrometer- and nanometer-sized TiC powder.

Slurry erosion happens extensively in the industries of mining, metallurgy, and crude-oil drilling. Materials with improved wear resistance to slurry erosion are in increased demand in industry. It is well known that hard materials have a high erosion resistance at a low-impact angle, while ductile materials have a high erosion resistance at a high-impact angle. However, in some service conditions, components suffer slurry erosion at varying impact angles. Therefore, it is of practical significance to develop coatings with an overall excellent erosion resistance, no matter what the impact angles are. Considering their good combination of hardness and ductility, steel matrix composites may be potential erosion-resistant materials at various impact angles. H13 is a die-cast steel having a good corrosion and erosion resistance. Recently, it was found that laser surface coating of TiC on a H13 tool steel improved the corrosion and erosion

* Corresponding author. Tel.: +1 214 768 4865; fax: +1 214 768 0812.
E-mail address: kovacevi@engr.smu.edu (R. Kovacevic).
[1] Present address: Department of Materials Science and Engineering, University of Tennessee, TN 37996, USA.

0924-0136/$ – see front matter © 2007 Elsevier B.V. All rights reserved.
doi:10.1016/j.jmatprotec.2006.12.053

resistance and consequently, prolonged the service life of die-cast dies [6,7]. Utilizing laser deposition processing, the present work seeks to develop TiC/H13 tool steel composite coatings as new erosion resistant materials.

Laser processing is characterized by high energy density, low heat input, and consequently, high heating and cooling rates that minimize its effect on a substrate. However, laser processing parameters such as beam power and scanning speed affect the metallurgical quality, microstructures, and furthermore, mechanical properties of coatings [8]. In this work, the laser deposition technique is used to synthesize TiC/H13 tool steel coatings with different concentrations of TiC. The effect of beam-scanning speeds on the microstructures of coatings is investigated for a given beam power and powder-feeding rate.

Slurry erosion is a rather complex process. Generally speaking, the factors affecting erosion can be divided into three classes, i.e., the properties of target materials, impingement particles, and test conditions. Much attention has been paid in studying slurry erosion of various materials [9–14]. Despite the fact that some relationships between the properties of some materials and erosion resistance have been recognized [13], individual materials demonstrated a great difference in erosion resistance in various environments. Therefore, a wear-resistant material needs to be identified in a simulating service condition.

The widely used Coriolis slurry erosion tester is designed to simulate particle sliding or a low-impact angle condition [15]. Since in the tester fluid flow is almost parallel to the surfaces of components, this tester is suitable to examine the erosion behavior of the materials of pipe wall. But, some critical components in the pumping system suffer the strong impact of fluid flow containing hard sand particles at angles from 0 to 90°. Therefore, a slurry jet erosion test at various impact angles is necessary.

The present work further investigates the slurry erosion resistance of the laser deposited TiC/H13 tool steel composite coatings at various impact angles and compares the results with resistance from a hard carbide coating and a low alloy steel.

2. Experimental procedure

An AISI 4140 steel plate was used as a substrate, the composition of which is shown in Table 1. The H13 tool steel powder was used as a matrix of composite coatings. The original size of the H13 tool steel powders is 50–100 μm. Its composition is also shown in Table 1. The original size of injected TiC particles is 50–100 μm. Three composite coatings with the nominal volume fractions of 40, 60, and 80% TiC were designed.

An Nd:YAG laser with a maximum power of 1 kW in continuous wave form was utilized to produce coatings. The beam power used in the experiments was 380 W, with a spot diameter of 1 mm. The beam-scanning speeds were set as 5.08, 7.62, 10.16, and 12.7 mm s^{-1}. A powder-feeding system was used for direct injection of powders into the molten pool with argon flow as a powder carrier. The TiC and H13 tool steel powders were injected by two powder feeders through four nozzles of 1 mm in diameter. The total powder feeding rate was fixed at 4 g min^{-1}. The TiC and H13 tool steel powders were premixed according to the designed constitutions of coatings. Single and double layer beads were deposited at various beam-scanning speeds. In the case of an overall coating, substrate samples (25.4 mm × 25.4 mm) were coated uniformly with double layers of about 1 mm in thickness. The beam-scanning speed was 10.16 mm s^{-1}. A 40% overlap of successive melting track was selected to produce a uniform coating on a substrate.

Table 1
Nominal chemical composition of steels used (wt.%)

Element	C	Cr	Mo	Mn	Si	Ti	Fe
4140	0.4	1.0	0.2	0.9	0.2	–	Balance
H13	1.9	4.3	1.5	0.8	0.2	5.2	Balance

The transverse cross sections of the deposited beads were cut for microstructural examination. The optical microscopy and electron microprobe with energy dispersive spectrometry (EDS) were used for microstructural observation and microanalysis of composition. X-ray diffraction with Cu Kα was performed to identify the phases in the coatings produced at the beam-scanning speed of 10.16 mm s^{-1}. Microhardness measurements were conducted along the cross sections of the coating layers using a Leitz Wetzlar microhardness tester with a load of 100 g.

The slurry erosion tester used for this experiment was similar to the Coriolis erosion tester except that the slurry jet tester has the possibility to change an impact angle of slurry impact. The chosen slurry jet tester utilized a centrifugal acceleration in a revolving rotor to push slurry that consists of water and sand rapidly onto a sample surface such that the solid particles are forced against the surface, producing wear during their impact. Duplicate samples were used in each erosion test. The samples were placed at a distance of 30 mm from the nozzles with possibility to change the angle of impact with respect to the slurry flow. Impact angles were changed from 30 to 90° with an increment of 15°. The rotational speed of the rotor used in all tests was 875 rpm, giving an impact speed of 25 m s^{-1}, onto sample surfaces. The slurry was made up of 12 wt.% spherical silica sand (SiO_2) in water. The hardness of the silica was about 750 HV with size between 425 and 850 μm. Each erosion test lasted 15 min. The specimen mass loss was measured, and, furthermore, erosion rate was calculated.

3. Results and discussion

3.1. Morphologies and microstructures of laser deposited coatings

Laser beam-scanning speeds affect the sizes and morphologies of the deposited beads. The typical morphologies of the cross sections of the beads produced at various beam-scanning speeds are shown in Fig. 1. It is well known that a laser-clad layer can be divided into three zones, i.e., build-up, dilution, and heat-affected zones in a substrate. A dilution zone refers to a melting zone within a substrate that consists of deposited material and substrate. A heat-affected zone is just beyond a dilution zone in a substrate, which experiences an elevated temperature, but does not melt. From Fig. 1, it can be seen that the build-up and dilution zones are influenced severely by the beam-scanning speeds. The faster the beam moves, the smaller the volume and the mass of the build-ups. Yet, the dilution zones decrease by decreasing the beam-scanning speeds and disappear completely at the minimal speed, i.e., 5.08 mm s^{-1}. It can be seen that only two intermediate beam-scanning speeds can develop good geometrical and symmetrical beads. At the maximum speed, 12.7 mm s^{-1}, the coating fails to coincide with the dilution zone; while at the minimal speed, the build-up tends to lean. It is noted that the maximum beam-scanning speed leads to the largest dilution zone but fails to homogenize it, as shown in Fig. 1d. This may result from both the larger dilution zone in the substrate and the higher solidification rate that mixed much substrate material with the deposited material. Double-layered depositions have the same dilution and heat-affected zones as the single ones. Undoubtedly, a double-layered deposition increases the thickness of the build-ups. Worthy to mention, the beads of

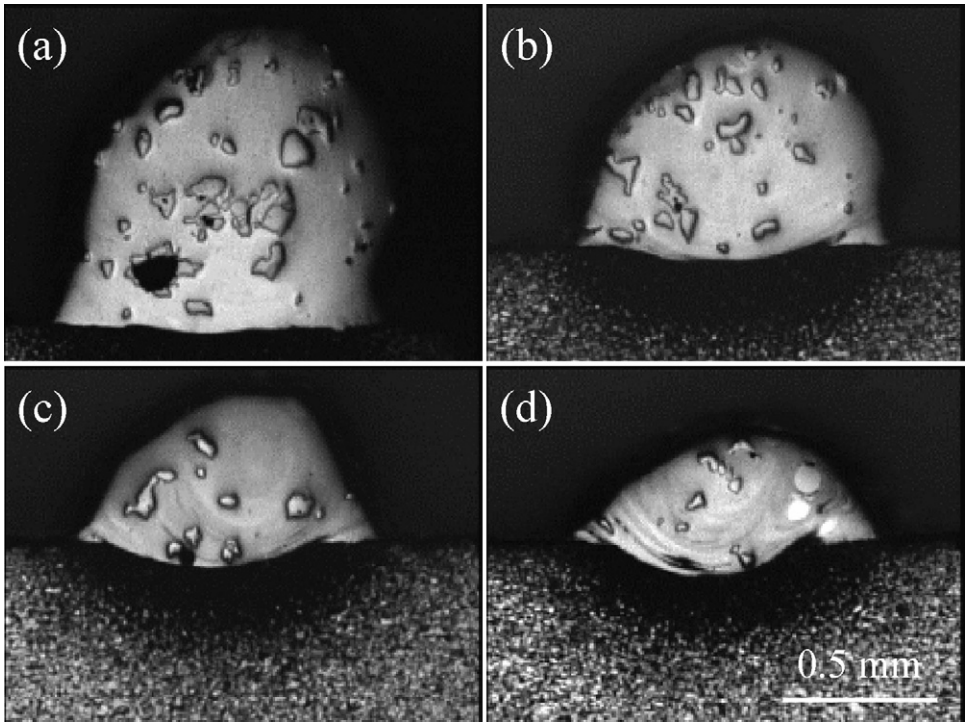

Fig. 1. Morphologies of beads of 60 vol.% TiC/H13 tool steel composite coatings formed by single layer scanning at speeds of (a) 5.08 mm s^{-1}, (b) 7.62 mm s^{-1}, (c) 10.16 mm s^{-1}, and (d) 12.7 mm s^{-1} and at a powder-feeding rate of 4 g min^{-1}.

the double-layered depositions at the minimal beam-scanning speed completely lose geometrical symmetry (Fig. 2).

From Fig. 1, it can be seen that the interface morphologies between a dilution zone and a heat-affected zone change with the beam-scanning speeds. By decreasing the beam-scanning speeds, their curvatures decrease. In the case of the minimal beam-scanning speed, a dilution zone disappears and the interface becomes planar. Fig. 3 shows typical high magnification micrographs of planar (at a speed of 5.08 mm s^{-1}) and curved (at a speed of 12.7 mm s^{-1}) interfaces. Evidently, the curved interface has a better melting bond than the planar.

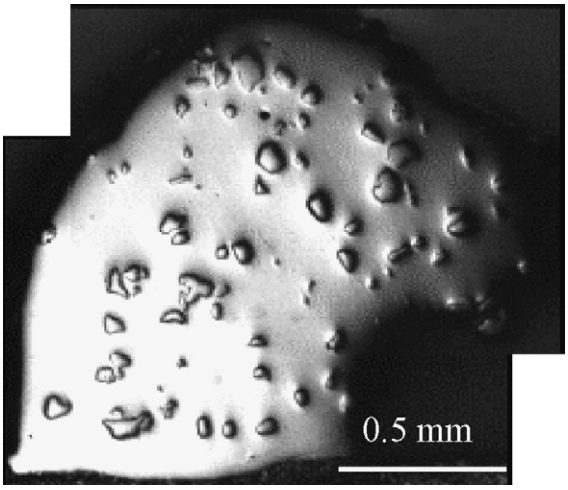

Fig. 2. Morphology of bead of 60 vol.% TiC/H13 tool steel composite coatings formed by double layer scanning at a speed of 5.08 mm s^{-1} and a powder-feeding rate of 4 g min^{-1}.

High magnification observation indicates that TiC particles decompose, and a great number of fine precipitates form during laser processing. For this reason, the injected coarse TiC particles in the beads appear fewer in the low magnification micrographs (Fig. 1). Fig. 4 shows the typical microstructures of the beads produced at various beam-scanning speeds.

For all the coatings, the fine precipitates are well distributed in steel matrices. Fig. 5 shows the backscattered electron images of the beads with 40, 60, and 80 vol.% TiC formed at the beam-scanning speed of 10.16 mm s^{-1}. In these images, both the coarse TiC and the fine precipitates appear dark, indicating that their constituting elements are lighter than the iron matrix. EDS demonstrated that fine precipitates are rich in Ti, as shown in Fig. 6. Furthermore, it can be seen that by increasing the amount of injected TiC, the fine precipitates increase both in quantity and size. The injected TiC particles exhibit clear, smooth edges and no reaction layer, indicating that they melt rather than dissolve during laser processing.

The morphologies and sizes of the fine precipitates are related to the concentrations of the injected TiC. Fig. 7 shows the fine precipitates in the beads with various concentrations of injected TiC produced at the beam-scanning speed of 10.16 mm s^{-1}. In 40 vol.% TiC, they assume substantially spherical and cubic shapes. In 60 vol.% TiC, some precipitates evolve into small flower-petal shapes, while the majority are still spherical. But, in 80 vol.% TiC, the precipitates are rather large and take spherical, cross, rod, and dendrite forms.

By a careful examination of Fig. 7b, it can be found that numerous fine precipitates are located at the center of the matrix grains. This indicates that they act as a solidified nucleus of the steel matrix grains.

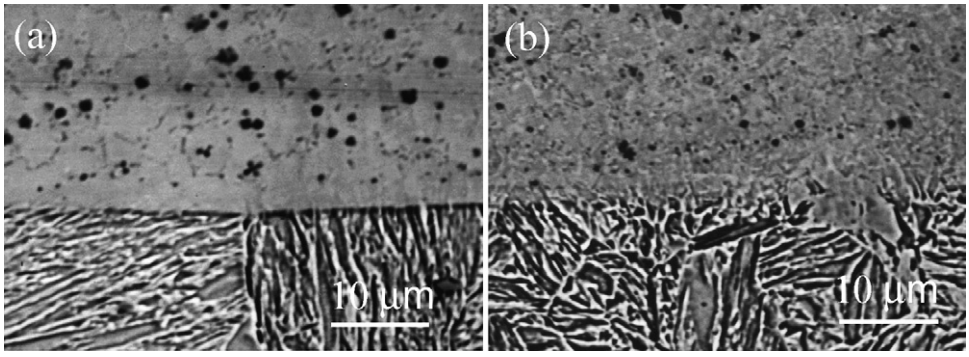

Fig. 3. High magnification micrographs of interfaces in 60 vol.% TiC/H13 tool steel composite coatings formed by single layer scanning at speeds of (a) 5.08 mm s^{-1} and (b) 12.7 mm s^{-1} and a powder-feeding rate of 4 g min^{-1}.

X-ray diffraction analysis was performed on the coatings with 40, 60, and 80 vol.% TiC produced at the beam-scanning speed of 10.16 mm s^{-1}, respectively. The resulting diffraction patterns are shown in Fig. 8. It can be seen that the diffraction patterns of all the coatings are similar, and there are only diffraction peaks of the steel matrix and TiC, indicating that TiC is only the second phase. These results mean that the fine precipitates are also TiC. The steel matrices are martensite and retained austenite.

The present results demonstrate that the sizes and morphologies of the deposited beads are closely related to a beam-scanning speed. During laser processing, laser energy is absorbed by both the fed powder and substrate. Undoubtedly, their proportion determines the morphologies of the beads. In the present work, the powder-feeding rate is constant and only a beam-scanning speed is varied. Therefore, heat input into the powder mixture and substrate changes depending on the beam scanning speeds. The faster the beam scanning speed, the less powder injected into the laser–powder interaction zone, and the more heat is input into the substrate. So, increasing a beam scanning speed results in a decreased deposited bead, but an increased dilution zone in a substrate.

At the minimal beam-scanning speed, the small melting zone in a substrate results in a weak interface bond between coating and substrate, as shown in Fig. 3a. Evidently, this speed is not suitable for producing coatings, not to mention the asymmetrical bead it produced (Figs. 1a and 2), that may accommodate gas and cause the formation of pores during overlapping in coating production. However, the maximum beam-scanning speed fails to make the upper build-up coincide properly with the lower dilution zone. More severely, some substrate material in a dilution zone does not mix well with the deposited materials (Fig. 1d). These disadvantages make the maximum beam-scanning speed

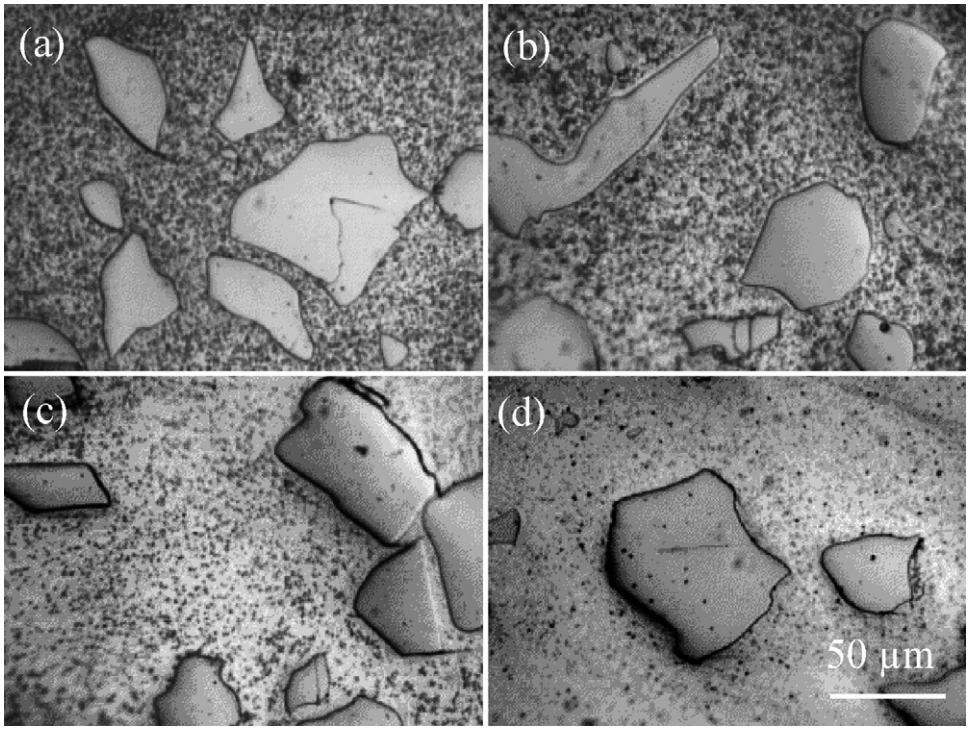

Fig. 4. Microstructures of 60 vol.% TiC/H13 tool steel composite coatings formed by single layer scanning at speeds of (a) 5.08 mm s^{-1}, (b) 7.62 mm s^{-1}, (c) 10.16 mm s^{-1}, and (d) 12.7 mm s^{-1} and a powder-feeding rate of 4 g min^{-1}.

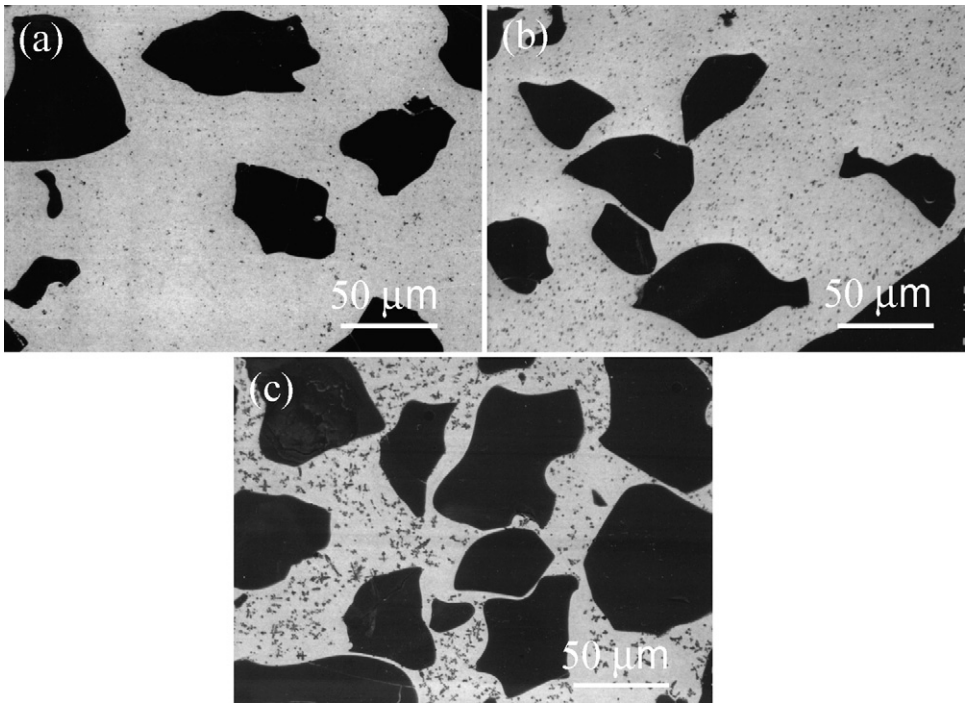

Fig. 5. Backscattered electron images (BEI) of (a) 40 vol.%, (b) 60 vol.%, and (c) 80 vol.% TiC/H13 tool steel composite coatings formed at a beam speed of 10.16 mm s^{-1} and a powder-feeding rate of 4 g min^{-1}.

unsuitable for producing coatings. From the viewpoint of the morphology of beads, both the maximum and minimal beam-scanning speeds are not ideal for coating production, while the intermediate beam-scanning speeds, 7.62 and 10.16 mm s^{-1} seem to be appropriate.

The smooth edges of the coarse TiC particles indicate that injected TiC melted rather than dissolved into the melt. As it is well known, a laser beam is characterized by a high energy density. The degree of absorption of the laser beam on metal and ceramic is very different. Ceramics have a much higher capability to absorb laser energy than metals. Therefore, in spite of its extremely high melting point (3140 °C) [6], the melting of TiC occurs during processing. As the laser processing time is extremely short, its melting is incomplete, and unmelted TiC remains.

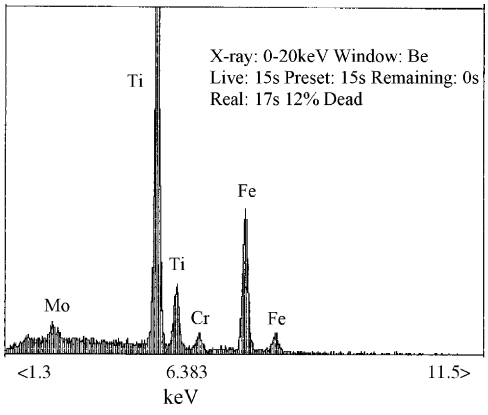

Fig. 6. Typical EDS of fine precipitates.

In all the coatings, fine TiC precipitates are uniformly distributed in the matrix. This distribution indicates that titanium and carbon atoms released by injected TiC are well distributed in the melts. Their homogeneous distribution must be attributed to vigorous convection caused by rapid heating of the laser beam. Rapid cooling leads to the transformation of a steel matrix into martensite (Fig. 8) that hardens the steel matrices. The fine precipitated TiC is observed to be a solidified nucleus of the steel matrix (Fig. 7b) that affects the refinement of the grain structures of the matrix. Undoubtedly, this favors the modification of solidified structures.

As it is well known, fine particles would improve the mechanical properties of composites. It is expected that the melting of coarse TiC and subsequent reprecipitation of fine TiC would impart better overall mechanical properties to coatings than the mechanical insertion of coarse TiC particles. Both the coarse remaining and the fine precipitated TiC particles are believed to have a clean interface with the steel matrix. As the original surface of injected TiC melts, a fresh surface is developed, and the fine TiC precipitates are formed in situ within the melts. Therefore, a stronger interface bond between TiC and the matrix may be achieved.

3.2. Hardness and erosion of the composite coatings

The hardness profiles along the depth of the overall coating layers are shown in Fig. 9. The hardness is a microhardness obtained only from the matrices of the composite coating, not including the contribution from coarse unmelted TiC. It can be seen that the hardness of the coating layers is up to 600–860 HV, much higher than that of the substrate, 200–250 HV. However,

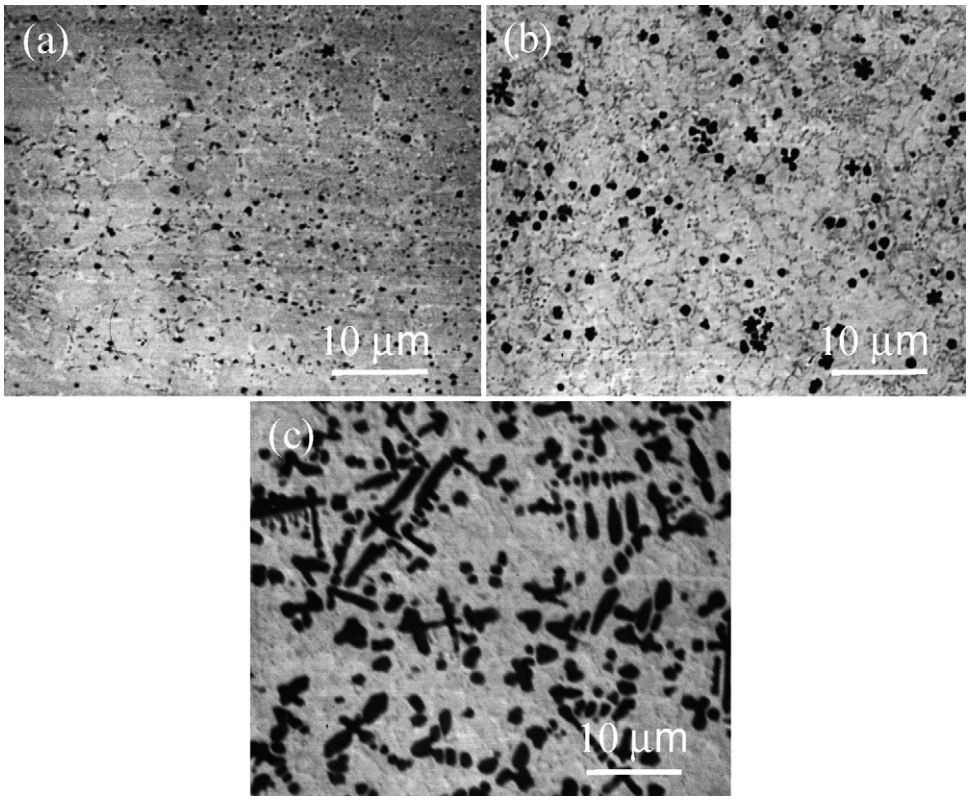

Fig. 7. High magnification BEI of (a) 40 vol.%, (b) 60 vol.%, and (c) 80 vol.% TiC/H13 tool steel composite coatings formed at a beam scanning of 10.16 mm s^{-1} and at a powder-feeding rate of 4 g min^{-1}.

there is a substantial difference in hardness among the three composite coatings. Evidently, by increasing the concentrations of TiC, the hardness increases, which is from more precipitation of fine TiC.

The erosion behavior of three TiC/H13 tool steel composite coatings was examined. Fig. 10 exhibits macrographs of the composite coatings eroded at various impact angles. It can be seen that impact angles affect the morphologies of the eroded scars substantially. At the higher impact angles (60 and 90°), the scars assume craters, while at the lower angles (30 and 45°), they are in the shape of a paraboloid. All the eroded scars are located at the center of the samples. This pattern indicates a good integrity of the erosion tester and guarantees the reliability of erosion data obtained.

Fig. 11 shows the slurry erosion rates of the coating layers at various impact angles. It can be seen that for all the composite coatings, the impact angles affect erosion rates substantially.

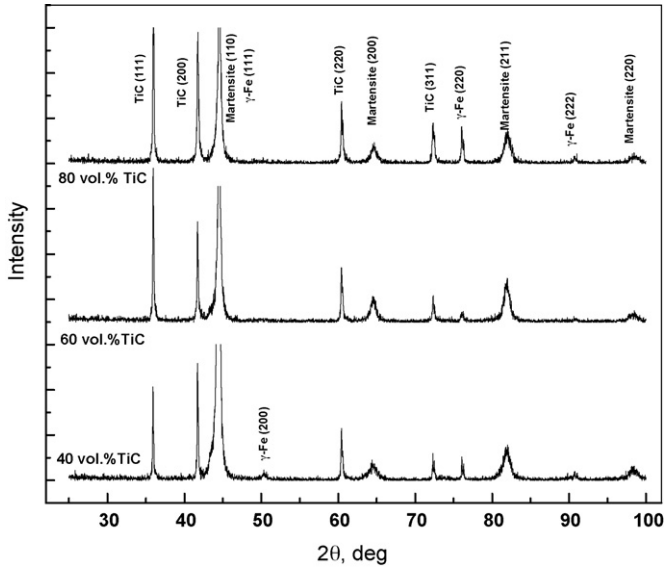

Fig. 8. X-ray diffractograms of 40, 60, 80 vol.% TiC/H13 tool steel composite coatings formed at a beam speed of 10.16 mm s^{-1} and at a powder-feeding rate of 4 g min^{-1}.

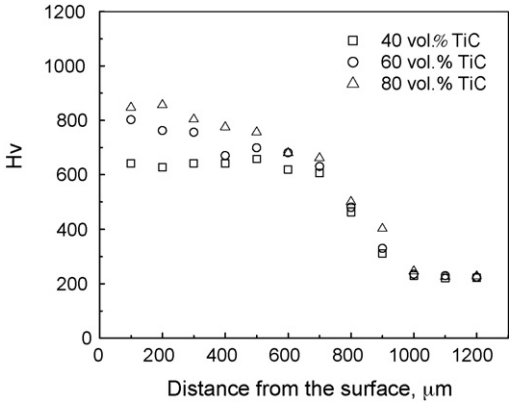

Fig. 9. Hardness profiles of 40, 60, 80 vol.% TiC/H13 tool steel composite coatings formed at a beam speed of 10.16 mm s^{-1} and at a powder-feeding rate of 4 g min^{-1}.

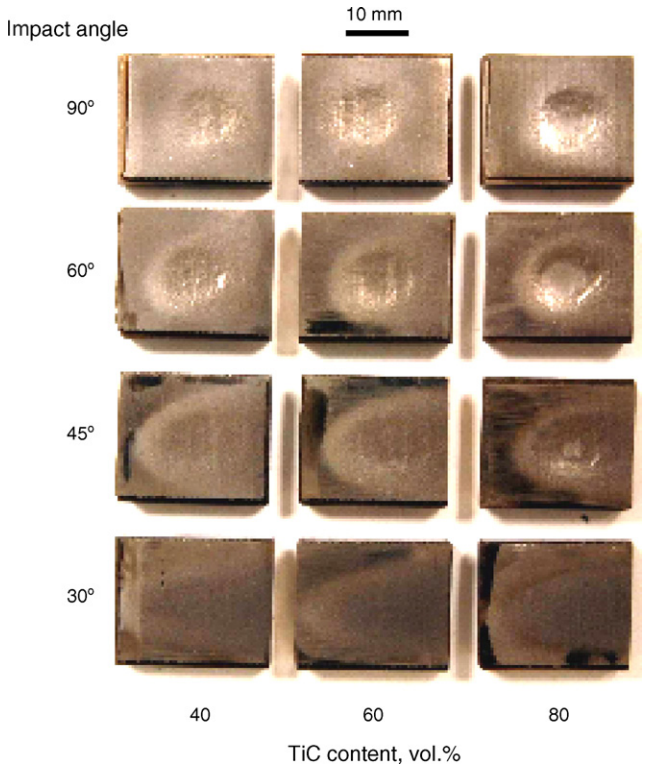

Fig. 10. Eroded samples of 40, 60, 80 vol.% TiC/H13 tool steel composite coatings (at a beam speed of 10.16 mm s^{-1} and a powder-feeding rate of 4 g min^{-1}) at various impact angles.

However, they exhibit similar characteristics. The smallest erosion rate is at an impact angle of 30°, the second smallest at 90°, and the most severe erosion happens at the intermediate impact angles, 45 and 60°. For the various impact angles, an erosion rate decreases by decreasing the concentrations of TiC in the coatings. The coating with 80 vol.% TiC has the lowest erosion resistance; while the coating with 40 vol.% TiC has the highest erosion resistance.

In order to evaluate the erosion resistance of the TiC/H13 tool steel composite coatings, the erosion rates of tungsten carbide

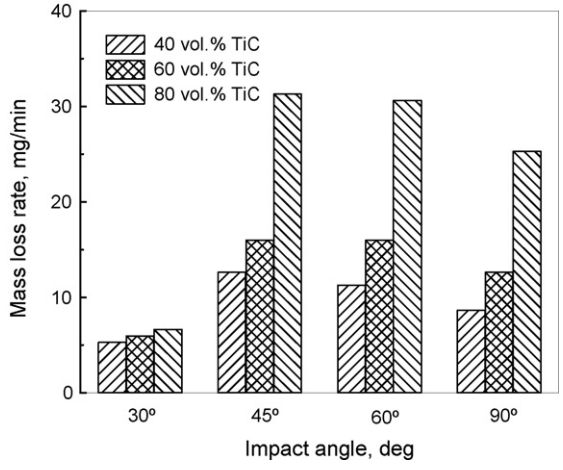

Fig. 11. Slurry erosion rates of 40, 60, 80 vol.% TiC/H13 tool steel composite coatings (at a beam speed of 10.16 mm s^{-1} and a powder-feeding rate of 4 g min^{-1}) at various impact angles.

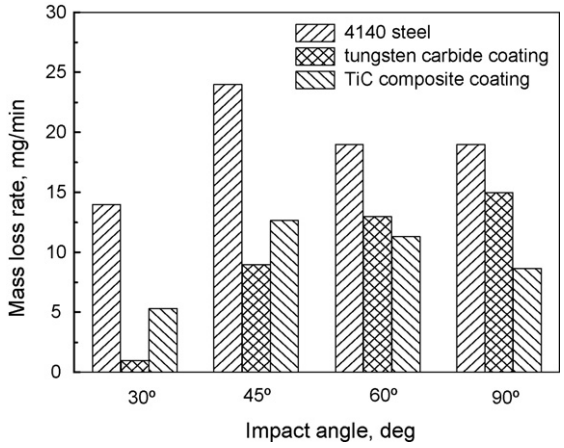

Fig. 12. Comparison of slurry erosion rates of 40 vol.% TiC/H13 tool steel composite coatings (at a beam speed of 10.16 mm s^{-1} and a powder-feeding rate is 4 g min^{-1}) with those of AISI 4140 steel and tungsten carbide coating.

coatings (hardness: 1000–1200 HV) and ductile AISI 4140 steel (hardness: 200–240 HV) at various impact angles [16] are compared with those of the coating with 40 vol.% TiC, as shown in Fig. 12. Evidently, the erosion rates of the hard tungsten carbide coatings increase with increasing impact angles and reach the maximum rate at an angle of 90°, while the ductile AISI 4140 steel suffers the most severe erosion at an angle of 45°. Such a characteristic feature is well known in a dry erosion, where ductile materials usually show greater wear at low angles while brittle materials tend to wear most at a normal impact [14,17]. However, it is reported that such trends are less clear in a slurry erosion [14]. The effect of impact angles on the erosion of materials must be related to the mechanical properties of the materials. For the composite coating with 40 vol.% TiC, the most severe erosion occurs at impact angles of 45 and 60°. This indicates that the composite coating may have a compromising mechanical property, i.e. better ductility than the hard tungsten carbide coating, and higher strength and hardness than AISI 4140 steel. Compared with the tungsten carbide coating and AISI 4140 steel, the developed composite coating with 40 vol.% TiC has a better erosion resistance. At all the impact angles, its erosion resistance is much higher than that of AISI 4140 steel. That demonstrates that low hardness of AISI 4140 steel makes it unsuitable for an application where erosion wear dominates. Although its erosion rates are higher than those of the tungsten carbide coating at lower impact angles, 30 and 45°, the erosion resistance of the composite coating is higher than those of the tungsten carbide coating at higher impact angles. Also, at the normal impact, it is only 57.8% of that of the tungsten carbide coating. Undoubtedly, the excellent erosion resistances of the composite coating at higher impact angles are attributed to its good ductility and toughness resulting from the H13 tool steel matrix.

The present work demonstrates that the laser deposited TiC/H13 tool steel composite coatings have an excellent erosion resistance, particularly at high erosion angles where the hard carbide coatings suffer the most severe erosion wear. The TiC/H13 tool steel composite coating is an alternate material for hard carbide coatings and has a potential application in an erosion service environment.

4. Conclusions

The results of the present study can be summarized as follows:

(1) The laser beam-scanning speeds affect the size and morphology of the deposited beads. The faster the beam moves, the larger the dilution zone, and the smaller the build-up zone.
(2) The higher beam-scanning speed fails to mix the deposited material properly with the substrate.
(3) During laser processing, TiC melts, decomposes, and subsequently, a number of fine TiC precipitates form and are distributed uniformly in the steel matrix.
(4) The amount of injected TiC has a strong impact on the morphology and size of the precipitated TiC. The larger the amount of the injected TiC, the larger in size the precipitated TiC. The larger TiC assumes spherical, rod, flower-petal shapes, and the form of dendrite; while the smaller TiC has spherical and cubic shapes.
(5) The TiC reinforcing composite coatings exhibit a decreased slurry erosion resistance at intermediate impact angles in the range from 0 to 90°; while at both lower and higher impact angles, they show an increased erosion resistance.
(6) By increasing the concentrations of TiC in the composite coatings, their erosion resistance decreases. The composite coating with 40 vol.% TiC shows an excellent erosion resistance.

Acknowledgements

The authors acknowledge the help of H.H. Mei, Z.G. Liu, M. Valant and P. Raige in execution of the experimental work.

References

[1] Q. Li, T.C. Lei, W.Z. Chen, Microstructural characterization of laser-clad TiC_p-reinforced Ni-Cr-B-Si-C composite coatings on steel, Surf. Coat. Technol. 114 (2–3) (1999) 278–284.
[2] Q. Li, T.C. Lei, W.Z. Chen, Microstructural characterization of WC_p-reinforced Ni-Cr-B-Si-C composite coatings, Surf. Coat. Technol. 114 (2–3) (1999) 285–291.
[3] J.H. Ouyang, Y.T. Pei, T.C. Lei, Y. Zhou, Tribological behavior of laser-clad TiC_p composite coating, Wear 185 (1–2) (1995) 167–172.
[4] S. Ariely, J. Shen, M. Bamberger, F. Dausiger, H. Hugel, M. Geller, Laser surface alloying of steel with TiC, Surf. Coat. Technol. 45 (1–3) (1991) 403–408.
[5] C. Tassin, F. Laroudie, M. Pons, L. Lelait, Carbide-reinforced coatings on AISI 316 L stainless steel by laser surface alloying, Surf. Coat. Technol. 77 (1–3) (1995) 450–455.
[6] W.P. Jiang, P. Mollan, Nanocrystalline TiC powder alloying and glazing of H13 steel using a CO_2 laser for improved life of die-casting dies, Surf. Coat. Technol. 135 (2–3) (2001) 139–149.
[7] D. Pirzada, E.G. Baburaj, R. Govindaraju, F.H. Froes, Laser surface coating of TiC on H13 die steel: effects on corrosion and erosion behaviour, Surf. Eng. 16 (2) (2000) 164–168.
[8] M. Riabkina-Fishman, E. Rabkin, P. Levin, N. Frage, M.P. Dariel, A. Weisheit, R. Galun, B.L. Mordike, Laser produced functionally graded tungsten carbide coatings on M2 high-speed tool steel, Mater. Sci. Eng. A A302 (1) (2001) 106–114.
[9] H.McI. Clark, R.B. Hartwich, A re-examination of the 'particle size effect' in slurry erosion, Wear 248 (1–2) (2001) 147–161.
[10] M. TaliaA, H. Lankarani, J.E. Talia, New experimental technique for the study and analysis of solid particle erosion mechanisms, Wear 229 (1999) 1070–1077.
[11] R. Dasgupta, B.K. Prasad, A.K. Jha, O.P. Modi, S. Das, A.H. Yegneswaran, Slurry erosive wear characteristics of a hard faced steel: effect of experimental parameters, Wear 213 (1–2) (1997) 41–46.
[12] H.W. Hoppel, H. Mughrabi, H.-G. Sockel, S. Schmidt, G. Vetter, Hydroabrasive wear behaviour and damage mechanisms of different hard coatings, Wear 229 (1999) 1088–1099.
[13] H.McI. Clark, R.J. Llewellyn, Assessment of the erosion resistance of steels used for slurry handling and transport in mineral processing applications, Wear 250 (2001) 32–44.
[14] H.M. Hawthorne, B. Arsenault, J.P. Immarigeon, J.G. Legoux, V.R. Parameswaran, Comparison of slurry and dry erosion behaviour of some HVOF thermal sprayed coatings, Wear 229 (1999) 825–834.
[15] H.M. Hawthorne, Some Coriolis slurry erosion test developments, Tribol. Int. 35 (10) (2002) 625–630.
[16] W.H. Jiang, P. Boussier, R. Kovacevic, unpublished work.
[17] I. Finnie, Some reflections on the past and future of erosion, Wear 186 (1) (1995) 1–10.